Author for correspondence:
Dr Naail Al Zuhir, Department of Radiology, Freeman Hospital, Freeman Road, Newcastle upon Tyne NE7 7DN, UK
E-mail: naail.alzuhir@nhs.net

Magnetic resonance non-echo planar diffusion-weighted imaging accuracy in detecting cholesteatoma in comparison with clinical and surgical findings

N Al Zuhir[1], I Zammit-Maempel[1], P Yates[2] and J Dixon[1]

Departments of [1]Radiology and [2]ENT, Newcastle upon Tyne Hospitals, Newcastle upon Tyne, UK

Abstract

Objective. Magnetic resonance imaging utilising non-echo planar diffusion-weighted imaging is known to have high sensitivity and specificity in detecting cholesteatoma.

Method. Data was retrospectively collected from patients who had undergone non-echo planar diffusion-weighted imaging from 1 January 2010 to 31 December 2016. The ratio of average pixel grey-scale values between the middle-ear lesion, pons and temporal lobe was used to quantify the degree of restricted diffusion and assess the statistical significance to detect cholesteatoma.

Results. A total of 107 patients had non-echo planar diffusion-weighted imaging during the study period. Non-echo planar diffusion-weighted imaging shows good specificity and sensitivity with an excellent positive predictive value and accuracy. Analysis of the grey-scale pixel ratio for cholesteatoma detection showed statistically significant results.

Conclusion. Non-echo planar diffusion-weighted magnetic resonance imaging is accurate for cholesteatoma assessment. When the middle-ear lesion non-echo planar diffusion-weighted imaging intensity is higher than the ipsilateral temporal lobe, it is highly suggestive of a cholesteatoma formation.

Introduction

Cholesteatoma formation in the middle ear happens as a consequence of keratin accumulation within a retraction pocket, which can aggressively progress to erode adjacent bones and middle-ear ossicles. This can lead to conductive hearing loss and other intra-temporal complications such as facial nerve palsy and sensorineural hearing loss, and intracranial complications including meningitis and abscess formation.

Cholesteatoma can be congenital or acquired. Acquired cholesteatoma occurs in two variations related to the site of its formation: a more common pars flaccida version and a less common pars tensa version.[1] Treatment is usually surgical, but there is a low risk of recurrence and when this occurs it is usually within the first two years post-operatively with approximately 60 per cent of recurrences occurring within the first post-operative year.[2] Post-operative recurrence is identified by clinical examination, examination under anaesthesia or second-look surgery if clinical examination is difficult or inconclusive.[3]

Several articles published in the literature are now advocating the use of magnetic resonance imaging (MRI) with non-echo planar diffusion-weighted imaging to detect primary cholesteatoma and post-operative recurrence because it has been shown to have a high specificity and sensitivity.[4,7] A current radiological dilemma for the diagnosis of cholesteatoma on non-echo planar diffusion-weighted imaging is the indeterminate high signal at the site of concern, with various suggestions in the literature to help with making a diagnosis, such as using apparent diffusion coefficient map images and T1-weighted images.[5,6,8]

Pixel-based signal intensity threshold technique for diffusion-weighted imaging has been used to assess prognosis in stroke patients by measuring a ratio between the area of restricted diffusion and another region of normal tissue in an attempt to quantify the degree of restricted diffusion.[7] Our study attempted to use the same technique with the aim of quantifying the degree of restricted diffusion within middle-ear lesions and assess its statistical significance.

Materials and methods

We performed a retrospective data collection for all patients with a clinical request questioning the presence of a primary or recurrent cholesteatoma who had non-echoplanar diffusion-weighted imaging MRI as part of MRI of the brain or internal auditory meatus between 1 January 2010 and 31 December 2016. CareStream™ PACS imaging software search function was used to review clinical requests.
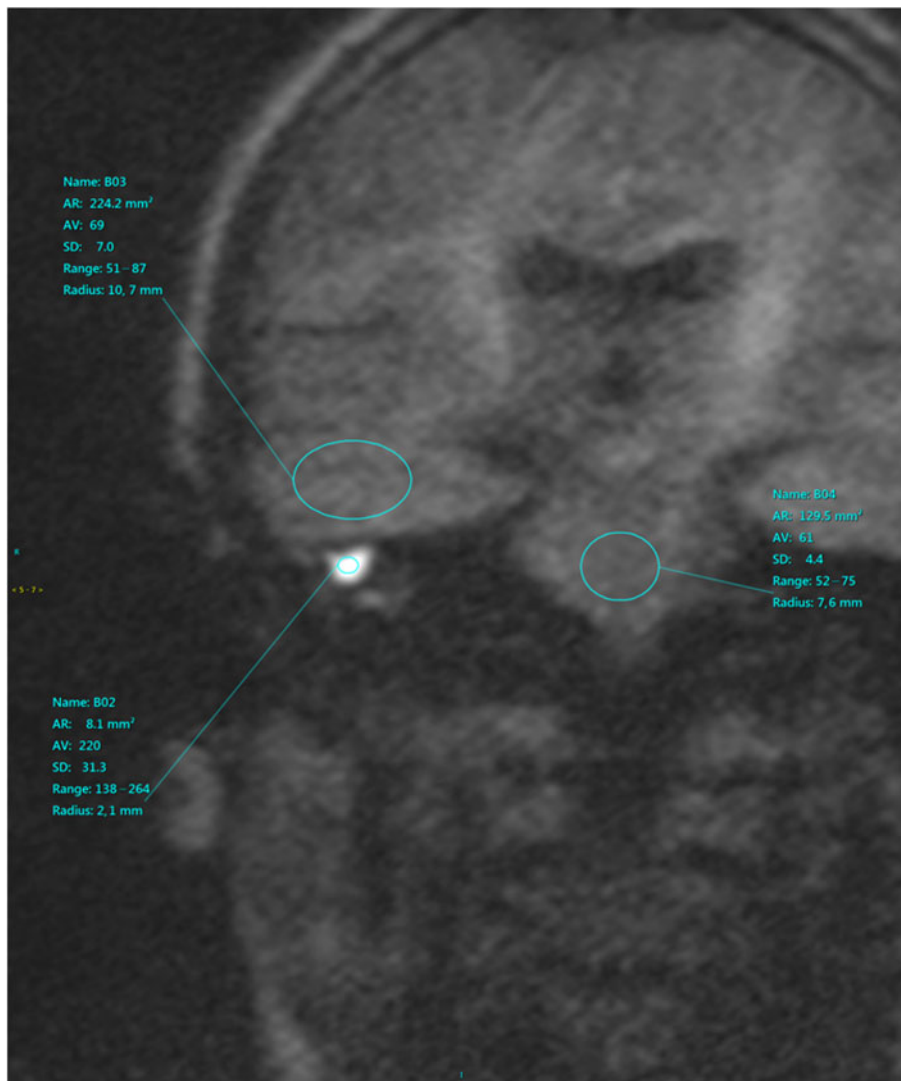
Fig. 1. Non-echo planar diffusion-weighted coronal image at the level of the middle-ear cleft showing the temporal lobes, pons and the middle-ear lesion. The middle-ear lesion, ipsilateral temporal lobe and pons were encircled using the region-of-interest tool in CareStream PACS software to obtain the average grey-scale value (AV) with standard deviation (SD) at these areas (AR). Region-of-interest radius measured across the temporal lobe and the pons were consistent in all cases whereas the middle-ear lesion region-of-interest radius depends on the size of the lesion itself.

Recorded data included demographic information, MRI findings, clinical examination or operative findings, interval between MRI and surgical intervention (if performed), and correlation between MRI and clinical or surgical findings. We excluded any patient who did not have clinical or surgical follow up.

MRI was performed on either Siemens Avanto[TM] or Symphony[TM] 1.5t MRI scanners with a cholesteatoma protocol that included: axial T2-weighted MRI scan of the brain, high-resolution volumetric T2-weighted MRI of the base of the skull, coronal T1-weighted MRI of the temporomastoid bone, coronal T2-weighted MRI of temporomastoid bone and coronal MRI of the temporomastoid bone with b1000 non-echo planar Haste[TM] diffusion-weighted imaging.

Sensitivity, specificity, positive predictive value, negative predictive value and accuracy were calculated using a contingency table.

Pixel-based signal intensity threshold was calculated as the average between grey-scale pixel value on non-echo planar diffusion-weighted imaging in the middle-ear lesion, pons and ipsilateral temporal lobe using the CareStream elliptical region-of-interest tool, circling the entire ipsilateral temporal lobe, pons and the high signal middle-ear lesion (Figure 1). We excluded lesions that were smaller than 3 mm because these cannot be adequately assessed using the region-of-interest tool (Figure 2).

Statistical analysis was performed on the average grey-scale pixel value ratio between the lesion and ipsilateral temporal lobe and between the lesion and pons with the Mann–Whitney U test using SPSS® statistical software (version 19). Receiver operating characteristic curve analysis was performed with the aim to identify a cut-off point in the ratio measured to confidently diagnose cholesteatoma. Patients with no lesion to measure were excluded from the statistical analysis.

Results

We identified 107 patients who had a non-echo planar diffusion-weighted MRI in the study period with a clinical question regarding the presence of primary or recurrent cholesteatoma on the clinical request card.

We excluded 8 patients: 7 had a middle-ear lesion of less than 3 mm on non-echo planar diffusion-weighted imaging MRI and 1 patient did not have clinical or surgical follow up after the MRI results.

Average age was 44 years (± standard deviation (SD), 22 years). There were 40 patients (40 per cent) who were imaged after having a previous cholesteatoma surgical treatment, with 27 of these patients (27 per cent) having had the surgical intervention more than 2 years prior to performing the MRI study and with the remaining patients having had the surgical
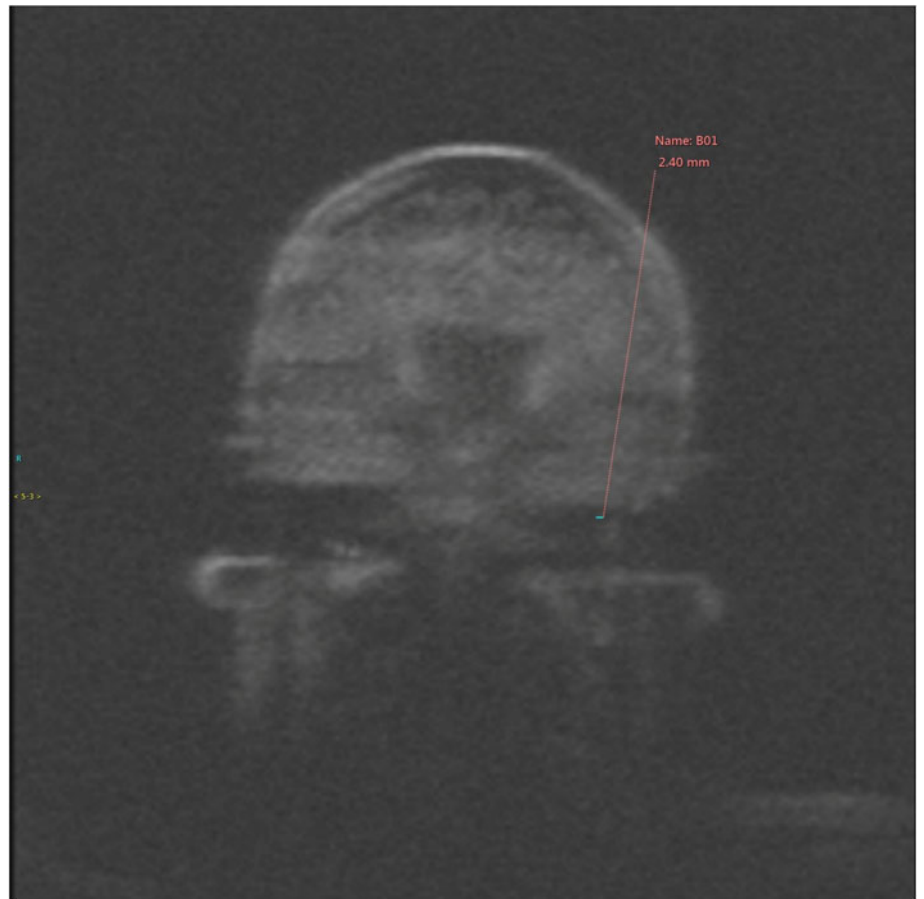
Fig. 2. Example of a middle-ear cleft lesion on coronal non-echo planar diffusion-weighted imaging which was smaller than 3 mm and therefore excluded from the study.

Fig. 3. Contingency table showing the true condition as the surgical or clinical diagnosis of cholesteatoma while the radiological diagnosis of cholesteatoma was considered as the predicted condition; the true positives and negatives and false positives and negatives are shown accordingly. Specificity, sensitivity, accuracy and predictive values were calculated from this contingency table.

intervention between 6 months and 1 year, 6 months prior to the study.

Using the contingency table (Figure 3), sensitivity was measured at 86 per cent, specificity was measured at 98 per cent, positive predictive value was 97 per cent, negative predictive value was 93 per cent and accuracy was measured at 94 per cent.

Pixel-based signal intensity threshold analysis was performed on 49 patients with measurable lesions as remaining patients had no measurable lesions on non-echo planar diffusion-weighted imaging (Figure 4). A total of 46 patients had concordant clinical and radiological diagnosis of the presence or absence of cholesteatoma.

Measurements of the ipsilateral temporal lobe and pons pixel-based intensity were very similar, and we elected to use the ipsilateral temporal lobe values to calculate the ratio for statistical analysis.

The Mann–Whitney U test was performed on the 46 patients with concordant surgical and radiological results (31 patients with a positive diagnosis of cholesteatoma and 15 patients with no cholesteatoma diagnosed), and a statistically significant difference was found in the means of the pixel-based signal intensity ratio of the lesion and the ipsilateral temporal lobe between the positive and negative diagnosis of cholesteatoma with $p < 0.05$ (95 per cent confidence interval (CI), -2.1278 to -1.0322 with equal variances assumed; Figure 5).

Further analysis for the surgical cholesteatoma diagnosis subgroup of 49 patients (33 patients with positive diagnosis of cholesteatoma and 16 patients with no cholesteatoma diagnosed) also showed a statistically significant difference in the
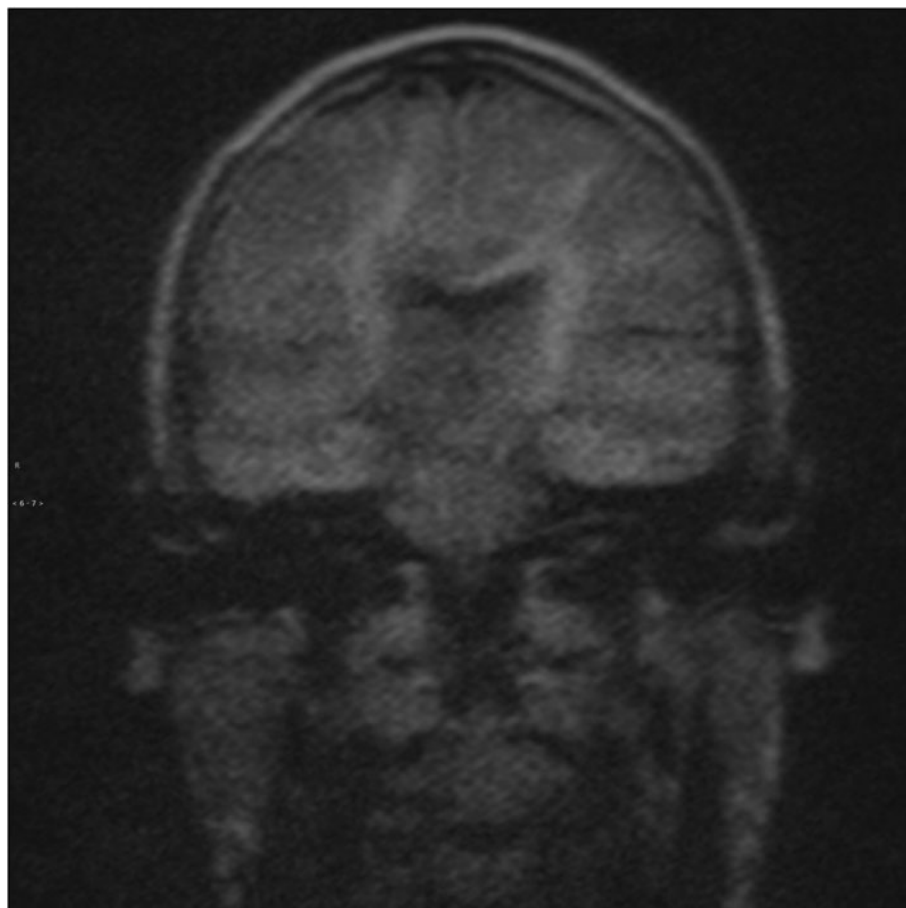
Fig. 4. Example of normal appearance of the middle-ear cleft on coronal non-echo planar diffusion-weighted imaging in which there was no lesion present to measure.
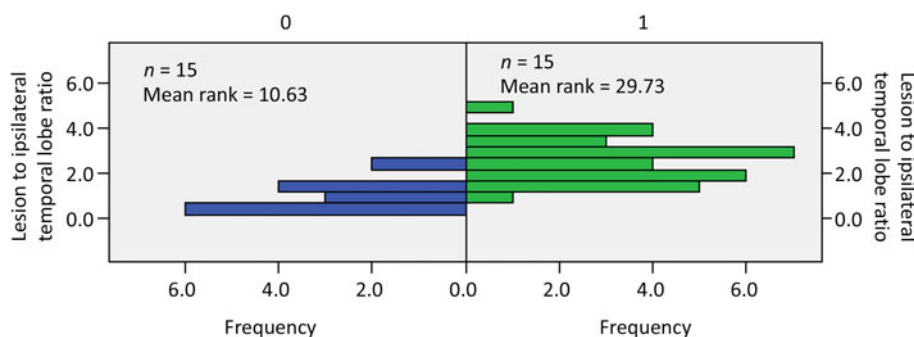

Fig. 5. Bar chart of independent samples Mann–Whitney U test showing the number of cases with concordant radiological and surgical diagnosis for cholesteatoma divided into two groups. Group 0 shows negative diagnosis and group 1 shows positive diagnosis with their respective ratio values of average grey-scale pixel intensity between the middle-ear cleft lesion and the ipsilateral temporal lobe (vertical axis) and the number of occurrences at these values (horizontal axis). Note the high ratio values in the positive group when compared with the negative group, with the difference in the ratio means between the two groups being statistically significant ($p < 0.05$).
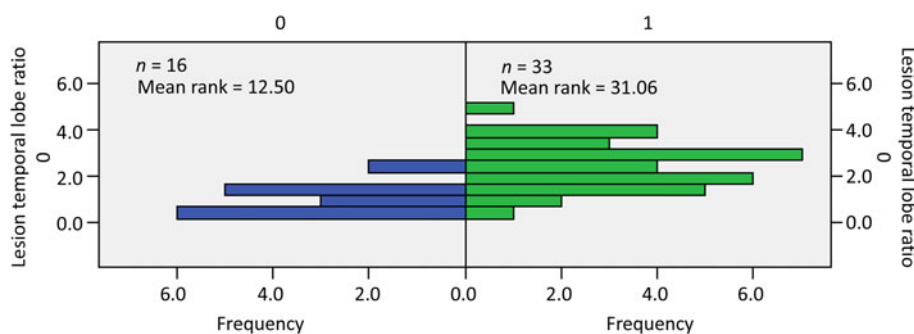
Fig. 6. Bar chart of independent samples Mann–Whitney U test showing the number of cases with surgical diagnosis for cholesteatoma divided into two groups. Group 0 shows negative diagnosis and group 1 shows positive diagnosis with their respective ratio values of average grey-scale pixel intensity between the middle-ear cleft lesion and the ipsilateral temporal lobe (vertical axis) and the number of occurrences at these values (horizontal axis). Note the high ratio values in the positive group when compared with the negative group, with the difference in the ratio means between the two groups being statistically significant ($p < 0.05$).

pixel-based intensity ratio with $p < 0.05$ (95 per cent CI, -1.9938 to -0.8624; Figure 6).

Further analysis of the radiological cholesteatoma diagnosis subgroup of 49 patients (32 patients with positive diagnosis of cholesteatoma and 17 patients with no cholesteatoma diagnosed) also showed a statistically significant difference in the

pixel-based intensity ratio with $p < 0.05$ (95 per cent CI, -2.1002 to -1.0726; Figure 7).

Receiver operating characteristic curve analysis was performed to assess a cut-off point in the ratio values for a surgical and radiological concordant diagnosis of cholesteatoma, and the ratio value found was 1.45 at 84 per cent sensitivity

Fig. 7. Bar chart of independent samples Mann–Whitney U test showing the number of the cases with radiological diagnosis for cholesteatoma divided into two groups. Group 0 shows negative diagnosis and group 1 shows positive diagnosis with their respective ratio values of average grey-scale pixel intensity between the middle-ear cleft lesion and the ipsilateral temporal lobe (vertical axis) and the number of occurrences at these values (horizontal axis). Note the high ratio values in the positive group when compared with the negative group, with the difference in the ratio means between the two groups being statistically significant ($p < 0.05$).
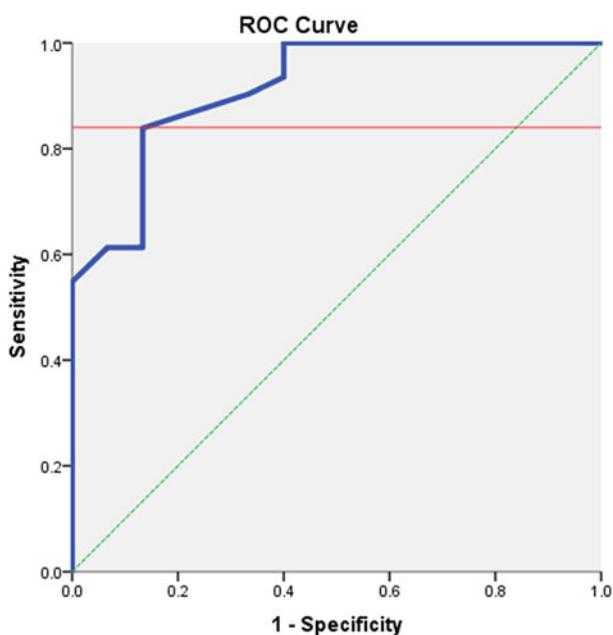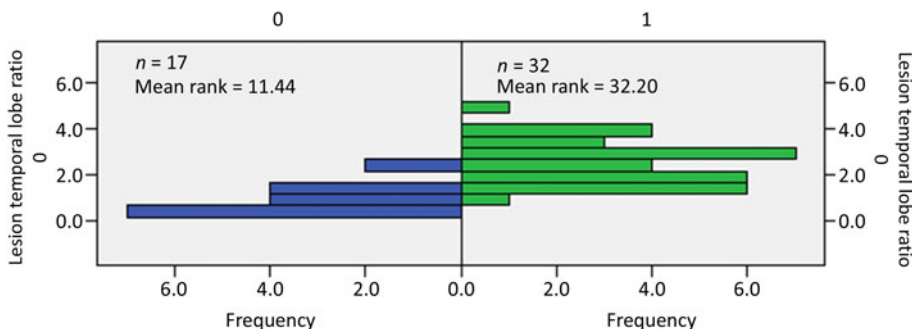

Fig. 8. Receiver operating characteristic curve chart with area under the curve corresponding to 0.915 (95 per cent confidence interval was 0.832 to 0.998) showing the cut-off level at 84 per cent sensitivity (red line) for the positive diagnosis of cholesteatoma which corresponds to an average grey-scale ratio value of 1.45 between the middle-ear cleft lesion and the ipsilateral temporal lobe. Note that the blocky curve is because of the small sample size which would bias the results.

and 98 per cent specificity with the area under the curve corresponding to 0.915 (95 per cent CI, 0.832 to 0.998). However, there was at least one tie between the positive and negative groups which biased the statistical analysis (Figure 8).

Discussion

Our study echoes other studies and meta-analyses published in the literature with comparable sensitivity and specificity.[4,6,7,10,11] Although other studies attempted to resolve the issues with indeterminate findings on diffusion-weighted images using other sequences like T1-weighted images and apparent diffusion coefficient map,[5,6] our study aimed to utilise the same sequence to interpret the findings (Figure 9). This was because acquiring an additional b0 value for a non-echo planar diffusion-weighted imaging sequence (to extrapolate an apparent diffusion coefficient map) would slightly increase the overall acquisition time of the study when there was no sufficient data in the literature at the period of our study data collection to suggest a significant unbiased statistical diagnostic value to obtain these sequences.[7,8]

Our study is limited by the low number of cases with a measurable lesion and an inherent bias of retrospective data collection for patients who had equivocal clinical and radiological findings which prompted an MRI scan. Despite this, the statistical analysis performed was conclusive with a cut-off point of the pixel-based intensity ratio between the measurable lesion in the middle ear and the ipsilateral temporal lobe at 1.45 to be suggestive of cholesteatoma formation. It is safe to assume that when the lesion identified in the middle-ear cleft on non-echo planar diffusion-weighted imaging is generally of higher signal intensity when compared with the ipsilateral temporal lobe or the pons, there is a high statistical probability to diagnose cholesteatoma. There were cases within the ratio region value between 1 and 1.9 with overlapping certainty of the radiological diagnosis of cholesteatoma which were either augmented by using a concurrent computed tomography (CT) scan or subsequently a decision whether to proceed with surgery based on the degree of clinical suspicion. In the majority of cases, those who went on to have surgery were confirmed to have cholesteatoma. One patient had surgery but did not have a cholesteatoma. Similarly, of those who were assessed clinically to be unlikely to have cholesteatoma, only one went on to have surgery at a later date for clinical reasons and subsequent non-echo planar diffusion-weighted imaging MRI confirmed cholesteatoma.

> • Non-echo planar diffusion-weighted imaging has high sensitivity, specificity and accuracy to detect cholesteatoma formation
> • Assessing the degree of diffusion restriction can be difficult in equivocal cases
> • Higher diffusion restriction ratio of the middle-ear lesion to the temporal lobe is suggestive of cholesteatoma formation

Out of 49 patients with measurable lesions, only 3 cases had discrepancy between the surgical and radiological diagnosis of cholesteatoma. Surgical intervention was performed more than six months after the MRI scan was performed in two of these cases, and only one case was a true false positive where adhesions and inflammatory tissue were found during surgery.

There is a certain learning curve for both the radiology department and the reporting radiologist in both reporting and performing these MRI studies with continued refinement of the scanning protocol. There was also an increase in confidence of the reporting radiologist over time, which was noted at our institute and while performing this retrospective study.[12]

Despite the current radiological workforce shortages in the UK as well as MRI capacity issues in most radiology departments, it would be more feasible to use MRI as an adjunct to clinical assessment rather than second-look surgery when

Fig. 9. Example of equivocal middle-ear cleft lesion signal intensity on coronal non-echo planar diffusion-weighted imaging that we are attempting to address with the aim of providing a way to identify which intensity is likely to represent a positive diagnosis for cholesteatoma. AV = average grey-scale value; SD = standard deviation; AR = areas

CT imaging is equivocal. Consideration needs to be made with regard to the cost and impact of second-look surgery on ENT departments to meet their other needs, and finding a balance between these two approaches would be the most appropriate way to assess cholesteatoma patients in the foreseeable future.[3,13]

Conclusion

Non-echo planar diffusion-weighted imaging MRI is a powerful and accurate tool to assess cholesteatoma when clinical findings or CT imaging are inconclusive or when recurrence is suspected.

Pixel-based signal intensity threshold analysis may play a role in equivocal cases as our study demonstrated that if the lesion in the middle-ear cleft has higher signal intensity when compared with the ipsilateral temporal lobe, there is high statistical probability of cholesteatoma diagnosis.

Competing interests. None declared

References

1 Rosito LS, Netto LF, Teixeira AR, Da Costa SS. Classification of cholesteatoma according to growth patterns. *JAMA Otolaryngol Head Neck Surg* 2016;**142**:168–72

2 Schwartz KM, Lane JI, Bolster BD, Neff BA. The utility of diffusion-weighted imaging for cholesteatoma evaluation. *AJNR Am J Neuroradiol* 2011;**32**:430–6

3 Crowson MG, Ramprasad VH, Chapurin N, Cunningham CD 3rd, Kaylie DM. Cost analysis and outcomes of a second-look tympanoplasty-mastoidectomy strategy for cholesteatoma. *Laryngoscope* 2016;**126**:2574–9

4 Muzaffar J, Metcalfe C, Colley S, Coulson C. Diffusion-weighted magnetic resonance imaging for residual and recurrent cholesteatoma: a systematic review and meta-analysis. *Clin Otolaryngol* 2017;**42**:536–43

5 Russo C, Elefante A, Di Lullo AM, Carotenuto B, D'Amico A, Cavaliere M et al. ADC benchmark range for correct diagnosis of primary and recurrent middle ear cholesteatoma. *Biomed Res Int* 2018;**2018**:7945482

6 Fukuda A, Morita S, Harada T, Fujiwara K, Hoshino K, Nakamaru Y et al. Value of T1-weighted magnetic resonance imaging in cholesteatoma detection. *Otol Neurotol* 2017;**38**:1440–4

7 De Foer B, Vercruysse JP, Bernaerts A, Meersschaert J, Kenis C, Pouillon M et al. Middle ear cholesteatoma: non-echo-planar diffusion-weighted MR imaging versus delayed gadolinium-enhanced T1-weighted MR imaging—value in detection. *Radiology* 2010;**255**:866–72

8 Lingam RK, Khatri P, Hughes J, Singh A. Apparent diffusion coefficients for detection of postoperative middle ear cholesteatoma on non-echo-planar diffusion-weighted images. *Radiology* 2013;**269**:504–10

9 Na DG, Thijs VN, Albers GW, Moseley ME, Marks MP. Diffusion-weighted MR imaging in acute ischemia: value of apparent diffusion coefficient and signal intensity thresholds in predicting tissue at risk and final infarct size. *AJNR Am J Neuroradiol* 2004;**25**:1331–6

10 She NN, Zhang XB. Diagnostic value of magnetic resonance imaging for middle ear cholesteatoma: a meta-analysis [in Chinese]. *Lin Chuang Erh Pi Yen Hou Ko Tsa Chih* 2017;**31**:1833–8

11 Cavaliere M, Di Lullo AM, Cantone E, Scala G, Elefante A, Russo C *et al*. Cholesteatoma vs granulation tissue: a differential diagnosis by DWI-MRI apparent diffusion coefficient. *Eur Arch Otorhinolaryngol* 2018;**275**:2237–43

12 Garcia-Iza L, Guisasola A, Ugarte A, Navarro JJ, Goiburu M, Altuna X. Utility of diffusion-weighted magnetic resonance imaging in the diagnosis of cholesteatoma and the influence of the learning curve. *Eur Arch Otorhinolaryngol* 2018;**275**:2227–35

13 Laske RD, Roth TN, Barath K, Schuknecht B, Huber AM, Roosli C. The role of non-echoplanar diffusion-weighted magnetic resonance imaging in diagnosis of primary cholesteatoma and cholesteatoma recidivism as an adjunct to clinical evaluation. *Ann Otol Rhinol Laryngol* 2018;**127**:919–25